Electronic Supplementary Material (ESI) for Catalysis Science & Technology.
This journal is © The Royal Society of Chemistry 2023

Supporting Information

High-throughput experimentation based kinetic modeling of selective hydrodesulfurization of gasoline model molecules catalyzed by $CoMoS/Al_2O_3$

E. Galand[a,b], F. Caron[a], E. Girard[a], A. Daudin[a], M. Rivallan[a], P. Raybaud[a], J.-M. Schweitzer[a], Y. Schuurman[b,*]

[a]IFP Energies nouvelles, Rond-point de l'échangeur de Solaize, BP3, 69360 Solaize, France

[b]IRCELYON, Univ Lyon, Université Claude Bernard Lyon 1, CNRS, 2 Avenue Albert Einstein F-69626, Villeurbanne, France

SI.1 Validation of the kinetic models

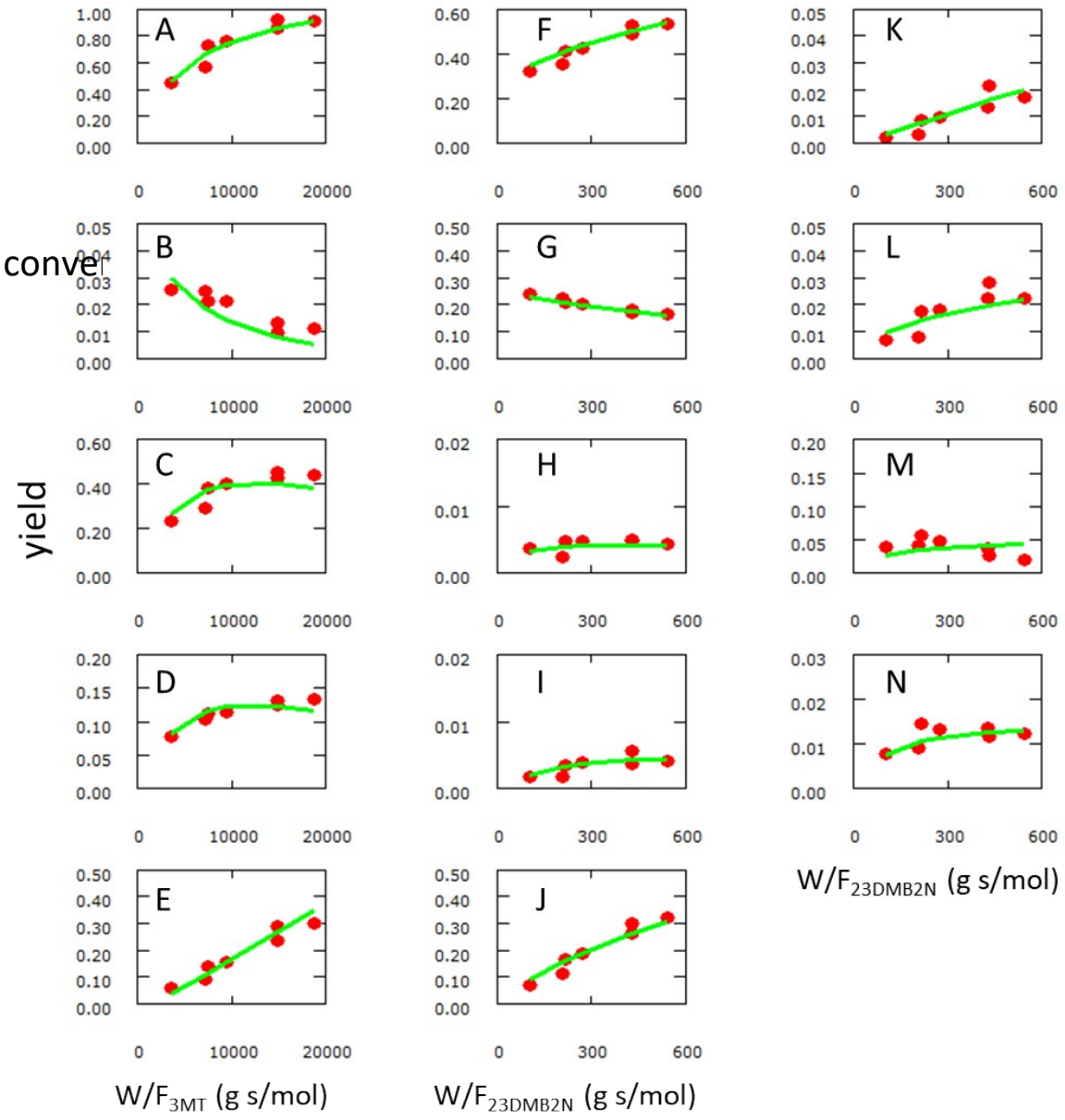

Figure S1. *Product yields from 3MT and 23DMB2N conversion over CoMo/Al_2O_3 (symbols: experiments, lines: model) as a function of W/F. A: 3MT (conversion), B: 3MTHT, C: 2MB2N, D: 2MB1N, E: 2MB, F: 23DMB2N (conversion), G: 23DMB1N, H: 33DMB1N, I: C6=, J: 23DMB, K: 22DMB, L: C12H24, M: 3MTC6, N: 3MTHTC6. 0.33 wt% 3MT, 10 wt% 23DMB2N, at 15 bar, H_2/feedstock ratio of 300 NL.L-1, 200-220°C*

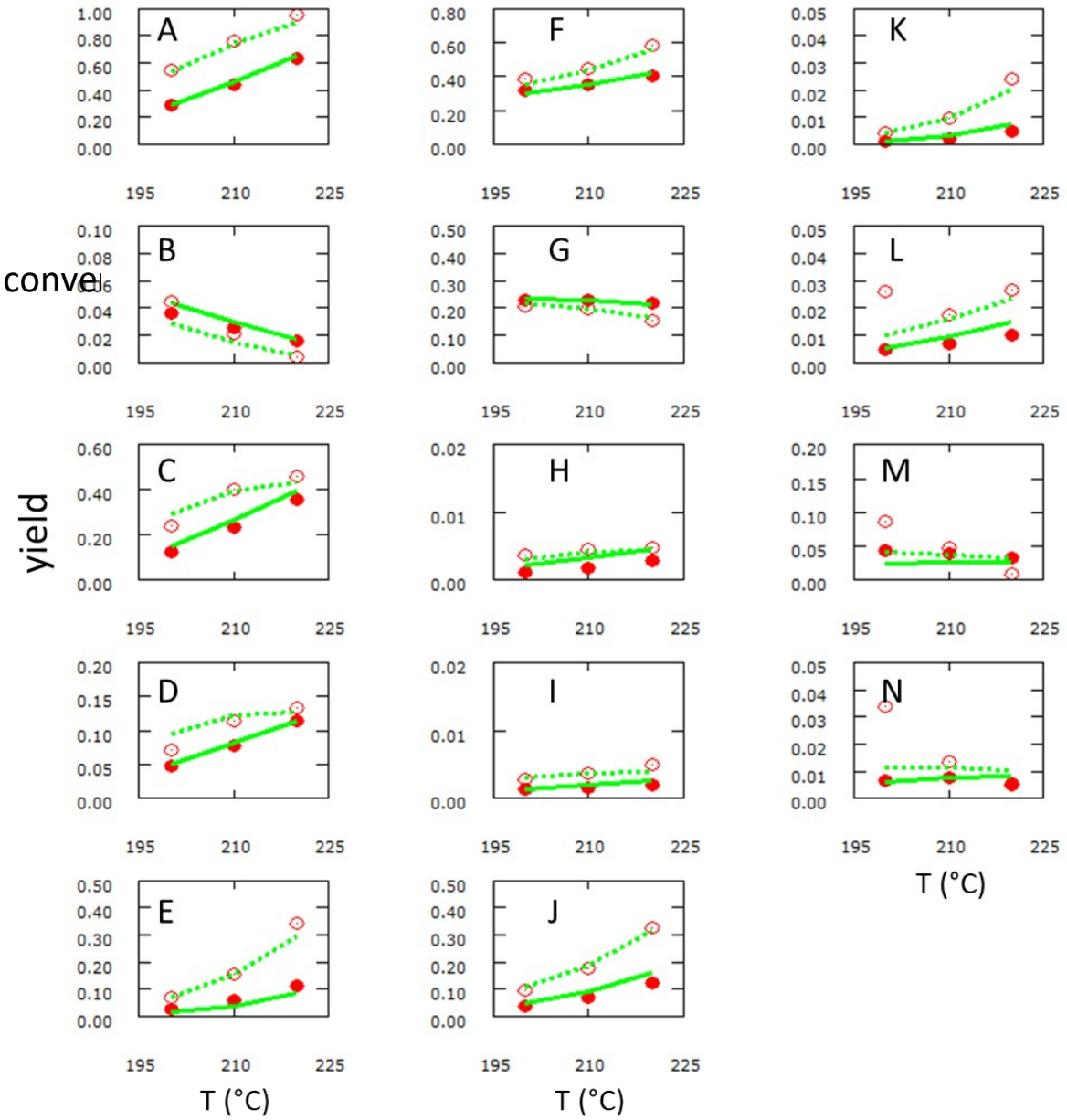

Figure S2. *Product yields from 3MT and 23DMB2N conversion over CoMo/Al_2O_3 at 15 bar, (symbols: experiments, lines: model) as a function of temperature at 2 different contact times (open symbols (3.6 10^6 g s mol^{-1}) /full symbols (9.4 10^6 g s mol^{-1}), dashed lines/full lines). A: 3MT (conversion), B: 3MTHT, C: 2MB2N, D: 2MB1N, E: 2MB, F: 23DMB2N (conversion), G: 23DMB1N, H: 33DMB1N, I: C6=, J: 23DMB, K: 22DMB, L: C12H24, M: 3MTC6, N: 3MTHTC6. 0.33 wt% 3MT, 10 wt% 23DMB2N, at 15 bar, LHSV of 3 h-1, H_2/feedstock ratio of 300 NL.L-1, 200-220°C*

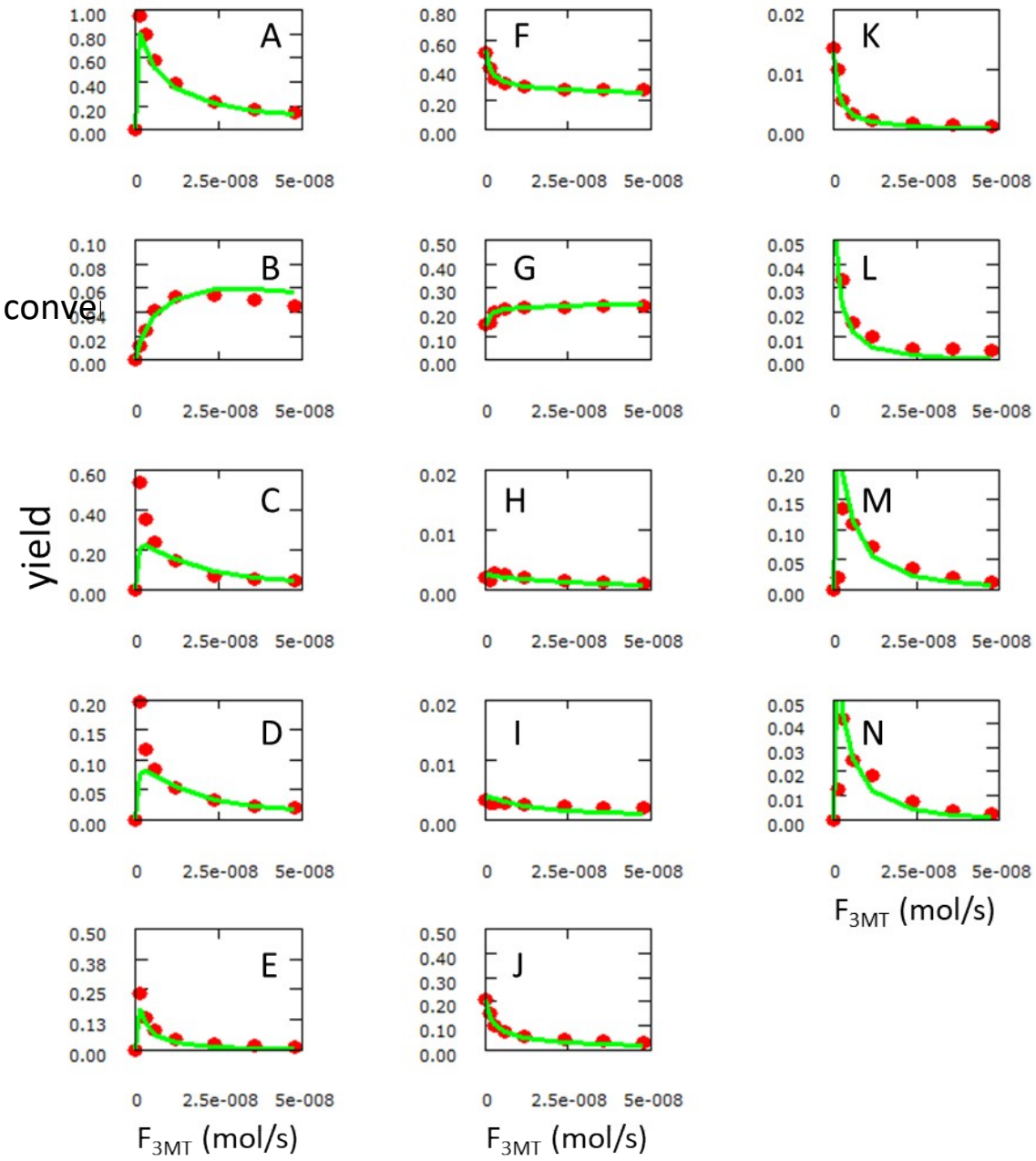

Figure S3. *Product yields from 3MT and 23DMB2N conversion over CoMo/Al_2O_3 at 15 bar, 180°C (symbols: experiments, lines: model)) as a function of the 3MT flow rate. A: 3MT (conversion), B: 3MTHT, C: 2MB2N, D: 2MB1N, E: 2MB, F: 23DMB2N (conversion), G: 23DMB1N, H: 33DMB1N, I: C6=, J: 23DMB, K: 22DMB, L: C12H24, M: 3MTC6, N: 3MTHTC6. 0 - 1.32 wt% 3MT, 10 wt% 23DMB2N over CoMo/Al2O3 at 15 bar, LHSV of 3 h-1, H_2/feedstock ratio of 300 NL.L-1, 180°C*

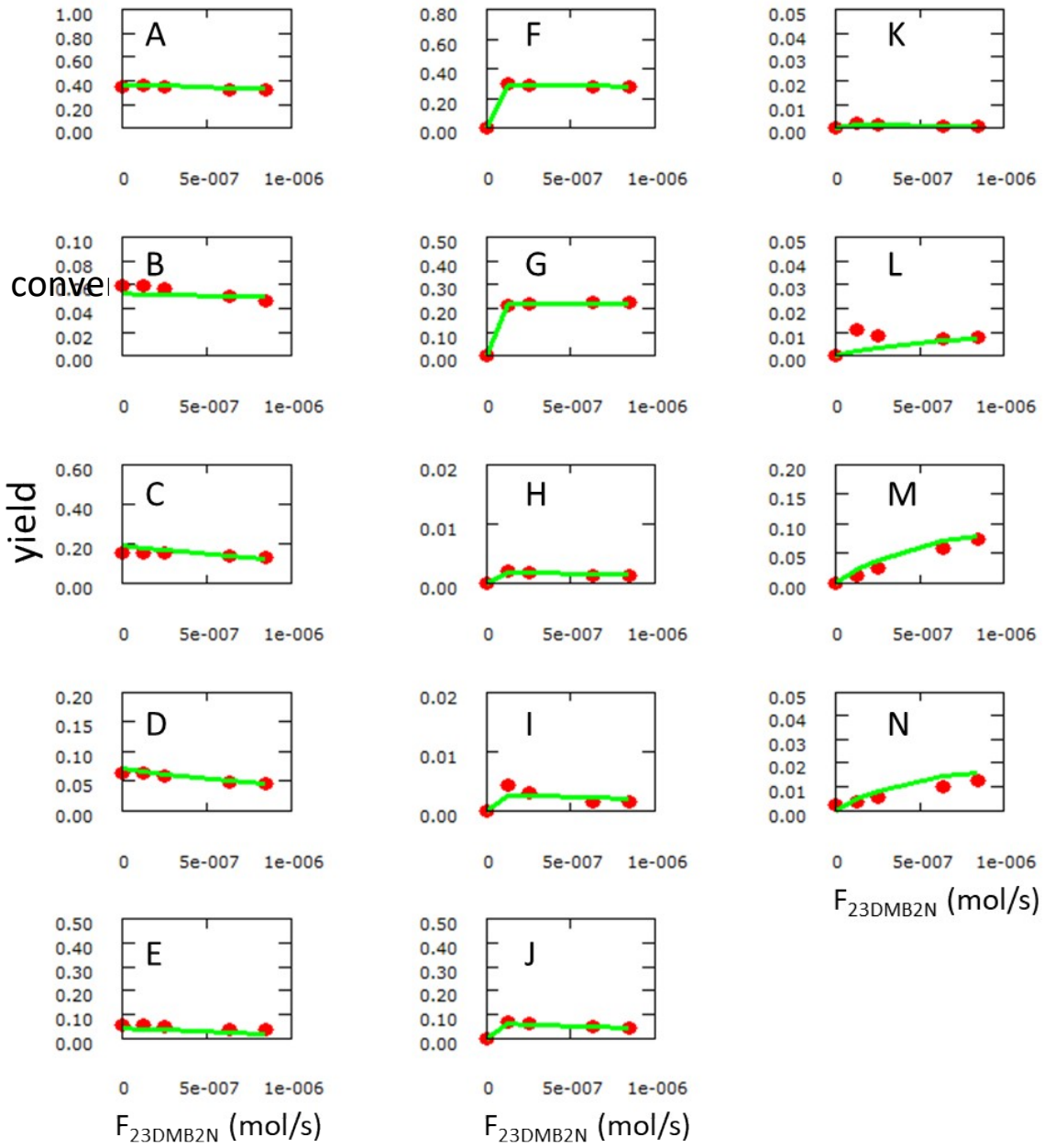

Figure S4. *Product yields from 3MT and 23DMB2N conversion over CoMo/Al_2O_3 at 15 bar, 180°C (symbols: experiments, lines: model)) as a function of the 23DMB2N flow rate. A: 3MT (conversion), B: 3MTHT, C: 2MB2N, D: 2MB1N, E: 2MB, F: 23DMB2N (conversion), G: 23DMB1N, H: 33DMB1N, I: C6=, J: 23DMB, K: 22DMB, L: C12H24, M: 3MTC6, N: 3MTHTC6. 0.33 wt% 3MT, 0-20 wt% 23DMB2N over CoMo/Al2O3 at 15 bar, LHSV of 3 h-1, H_2/feedstock ratio of 300 NL.L-1, 180°C*

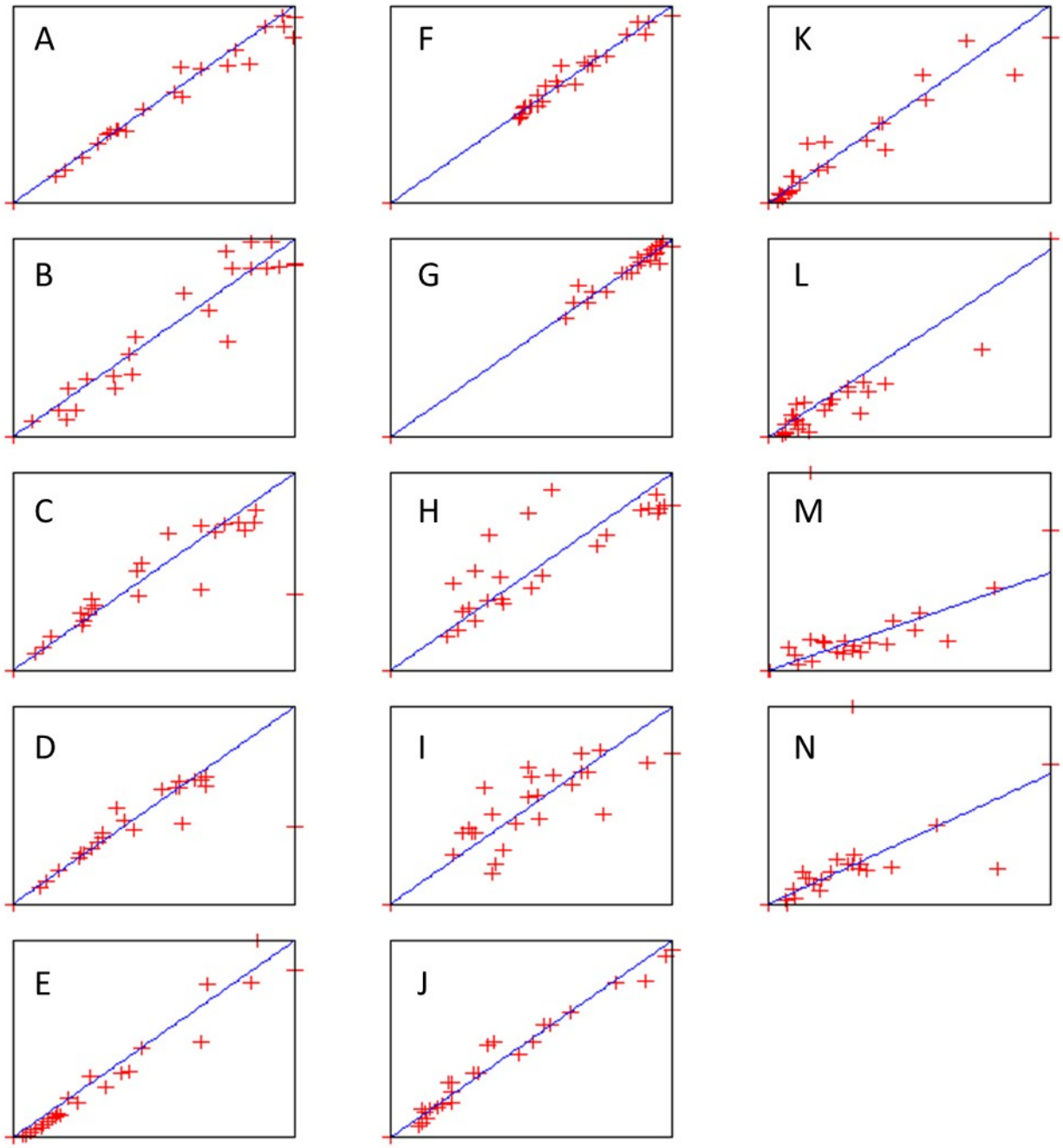

Figure S5. *Parity plots. A: 3MT, B: 3MTHT, C: 2MB2N, D: 2MB1N, E: 2MB, F: 23DMB2N, G: 23DMB1N, H: 33DMB1N, I: C6=, J: 23DMB, K: 22DMB, L: C12H24, M: 3MTC6, N: 3MTHTC6.*

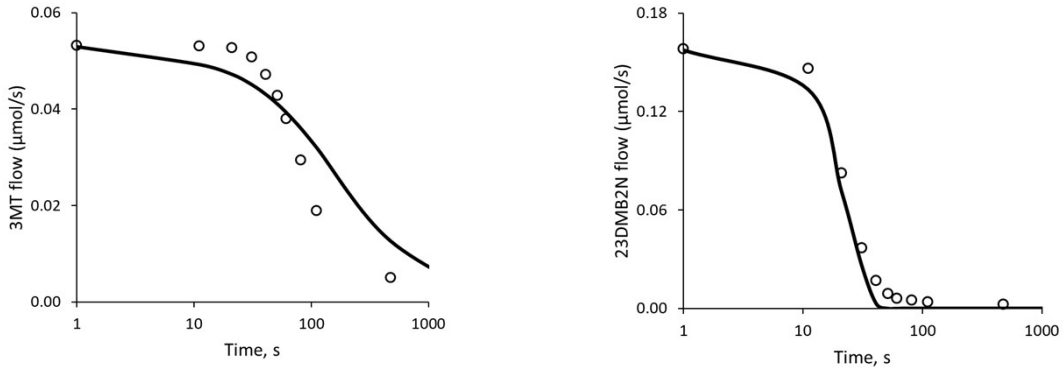

Figure S6. *Desorption experiments at 210°C and 1 bar total pressure over CoMo/Al_2O_3, symbols: experiments, line: model simulation based on the adsorption constants given in Table 3. Left desorption of 3MT, right desorption of 23DMB2N.*

Table S1. *Evaluation of different criteria to assess the intrinsic kinetic conditions.*

Physical phenomenon	**Criteria**
external mass transfer (Carberry number)	$5.7\ 10^{-2} < 0.1$
internal mass transfer (Wheeler-Weisz)	$0.15 < 0.33$
external heat transfer (film)	$0.01\ K < 1.8\ K$
external heat transfer (radial)	$0.006\ K < 1.7\ K$
internal heat transfer	$0.003\ K < 1.8\ K$

SI.2 Density functional theory (DFT) calculations

DFT calculations have been undertaken by using rigorously the same methodology as already described in great detail in Ref. [1]. We thus simply recall here some key parameters only. The total energy calculations are based on the plane wave density functional theory within the generalized gradient approximation [2,3]. We used the Vienna ab-initio simulation package [4,5] to solve the Kohn-Sham equations within the projected augmented wave formalism [6]. The cut-off energy governing the size of the plane wave basis set is fixed at 500.0 eV. The geometry optimization is completed when the convergence criteria on forces becomes smaller than 0.05 eV/Å. The supercell model used for simulating Co promoted slab is the same as in Ref. [1]. As in Ref. [7], we consider here the S-edge model containing 100% Co substituting Mo-atoms (Figure S7 a) and the M-edge model with 50% substitution of the Mo atoms by Co in a paired configuration (Figure S7 b). These edge structures have been previously determined as the relevant ones [1,7].

Figure S7 a) shows the optimized structures of H_2 dissociative adsorption on the fully Co promoted S-edge, leading to two SH species, corresponding to homolytic dissociation as assumed in equation (3) of the main text. H_2S dissociative adsorption on one vacancy site and on S-atom leading to 2 SH species as assumed in equation (4). Figure S7 b) illustrates similar molecular structures for the partially Co-promoted M-edge. The homolytic dissociation leading to 2 SH cannot be considered on this edge due to the presence of only one S on the edge per cell. In each case, we explore the various possible locations for H atoms (either on Mo and Co sites or on the various possible S sites, when they exist). Figure 7 reports the most stable configurations only. Regarding methyl-thiophene, and 2,3-dimethyl-butene, we used the same adsorption energy values as already reported in Refs. [1] and [7] for the same edges.

We recall that adsorption energies are calculated at 0 K as follows:

$$\Delta E = E(\text{edge} + \text{molecule}) - E(\text{edge}) - E(\text{molecule})$$

where E(edge), E(molecule) and E(edge+molecule) stands respectively for the electronic energies of the corresponding edge, the molecule (either H_2S or H_2) and the edge with adsorbed molecule.

These adsorption energies have been used in the kinetic model by assuming that $\Delta H°_{ads}$ is equal to ΔE in Table 2 of the main text.

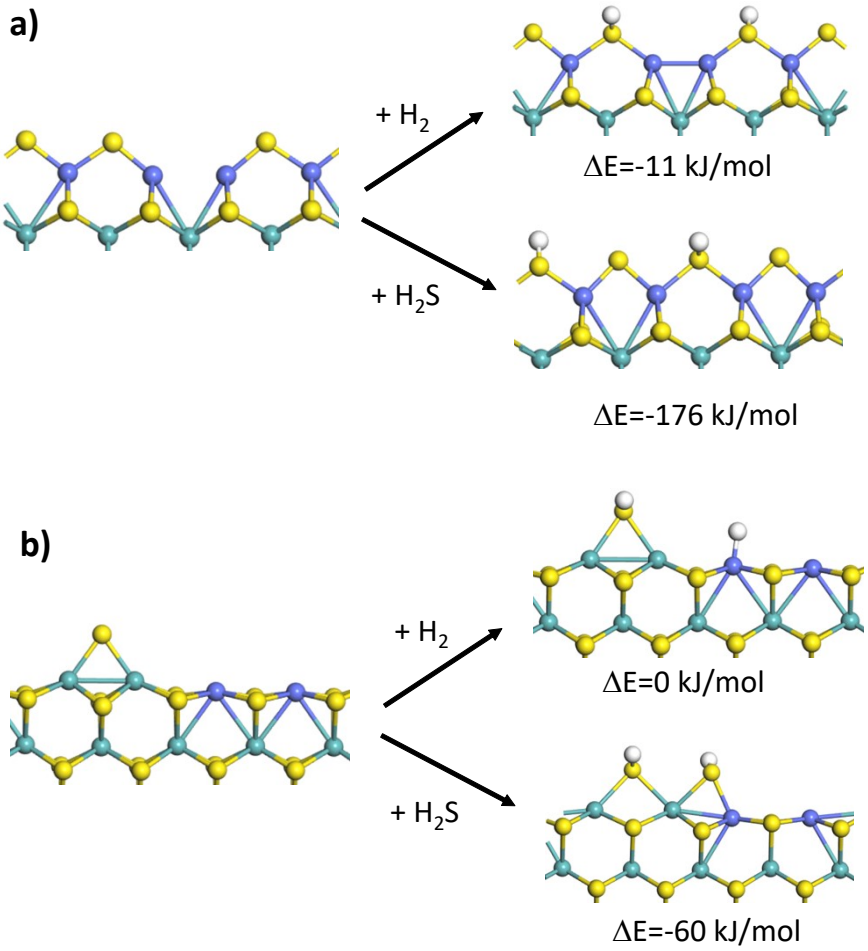

Figure S7. Molecular structures optimized by DFT calculations and corresponding adsorption energies for H_2 and H_2S: a) S-edge and b) M-edge. Color legend: yellow balls: S, green balls: Mo, blue balls: Co, white balls: H.

SI.3 Adsorption constants and rate constants for the Co-promoted M-edge

As explained in the manuscript to reduce parameter correlation, values of the adsorption enthalpies for the 4 adsorption steps used in the model were calculated by DFT for adsorption on the S-edge (main text) or M-edge (presented here, Table S2). Details are reported in [1,7]. The value of the adsorption entropy for the dissociative adsorption of hydrogen was fixed at -38 J/mol/K.

Table S2: *Values of the adsorption equilibrium constants, entropies and enthalpies for adsorption on the Co promoted M-edge. The values with ± 95% confidence intervals were estimated. All other parameters were fixed.*

Adsorption step		**K_i (bar^{-1}) 180°C**	**ΔS^0_{ads} (J/mol/K)**	**ΔH^0_{ads} (kJ/mol)**
1	XS	$(7 \pm 4)\ 10^3$	-199	-115[a]
2	O	5 ± 4	-141	-70[a]
3	H_2	0.01	-38[e]	0[b,c]
4	H_2S	$(1.3 \pm 0.7)\ 10^2$	-92	-60[b,d]

[a] DFT values reported in [1] and also used in [7] for XS=2 methyl-thiophene and O = 23DMB2N.

[b] DFT values determined on purpose by using the same periodic DFT formalism and same parameters as used in [1].

[c] For the M-edge with partial promotion of Co only heterolytic dissociation (MoH/CoH) of H_2 is calculated (for more detail, see SI.2).

[d] H_2S dissociatively adsorbed on one vacancy and on one S, leading to two adsorbed SH species as in equation (4) (for more detail, see SI.2).

[e] Corresponds to the loss of one degree of gas phase translation entropy, according to the Sackur-Tetrode equation [8].

Table S3: *Values of the parameter estimates for reaction on the M-edge with their 95% confidence intervals.*

Rate equation	k_i (180°C)	k_{-i} (180°) or K_i	E_a or ΔH_{iso} (kJ/mol)
5	$(1.1 \pm 0.1)\ 10^{-4}$		172 ± 6
6	$(3.5 \pm 0.2)\ 10^{-4}$		193 ± 6
7		$(3.6 \pm 0.1)\ 10^{-1}$	-10 ± 2†
8	$(3.6 \pm 0.7)\ 10^{-2}$		105 ± 8
9		$(3.10 \pm 0.01)\ 10^{-1}$	8 ± 1†
10	$(2.4 \pm 0.5)\ 10^{-4}$	$(3 \pm 2)\ 10^{-3}$	125 ± 7
11	$(9 \pm 3)\ 10^{-2}$	$(6 \pm 2)\ 10^{-2}$*	14 ± 5
12	$(9.6 \pm 0.2)\ 10^{-3}$		132 ± 5
13	$(5.4 \pm 0.1)\ 10^{-2}$		108 ± 8
14	$(5 \pm 2)\ 10^{-3}$		127 ± 11
15	$(1.2 \pm 0.2)\ 10^{-4}$		98 ± 12
16	$(4.1 \pm 0.7)\ 10^{-4}$		132 ± 13

† Reaction enthalpy (kJ/mol)

* Activation energy for the reverse step was fixed at $E_{a,forward}$ -8 kJ/mol.

SI.4 Model simulations

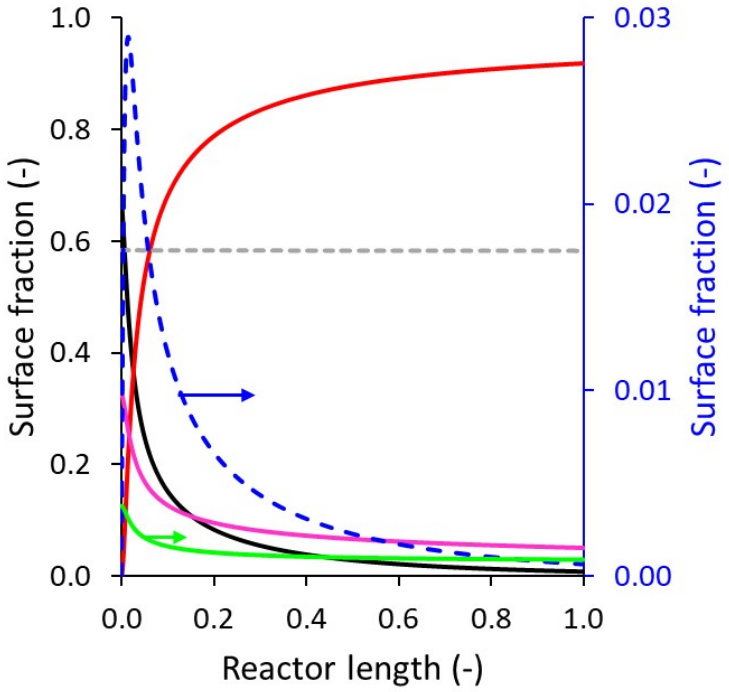

Figure S8. *Fractional surface coverage as a function of the catalyst bed length. 3MT conversion equals 0.95 at reactor outlet. Black full line θ_{3MT}, Red full line θ_S, Pink full line $\theta_{C6\_olefins}$, Grey dotted line θ_H, Blue dashed line θ_{3MTHT}, Green full line $\theta_{\#}$.* T=180°C, P_{H2}=10 bar, P_{3MT}=0.018 bar, $P_{23DM2BN}$=0.62 bar, X_{3MT}=0.95

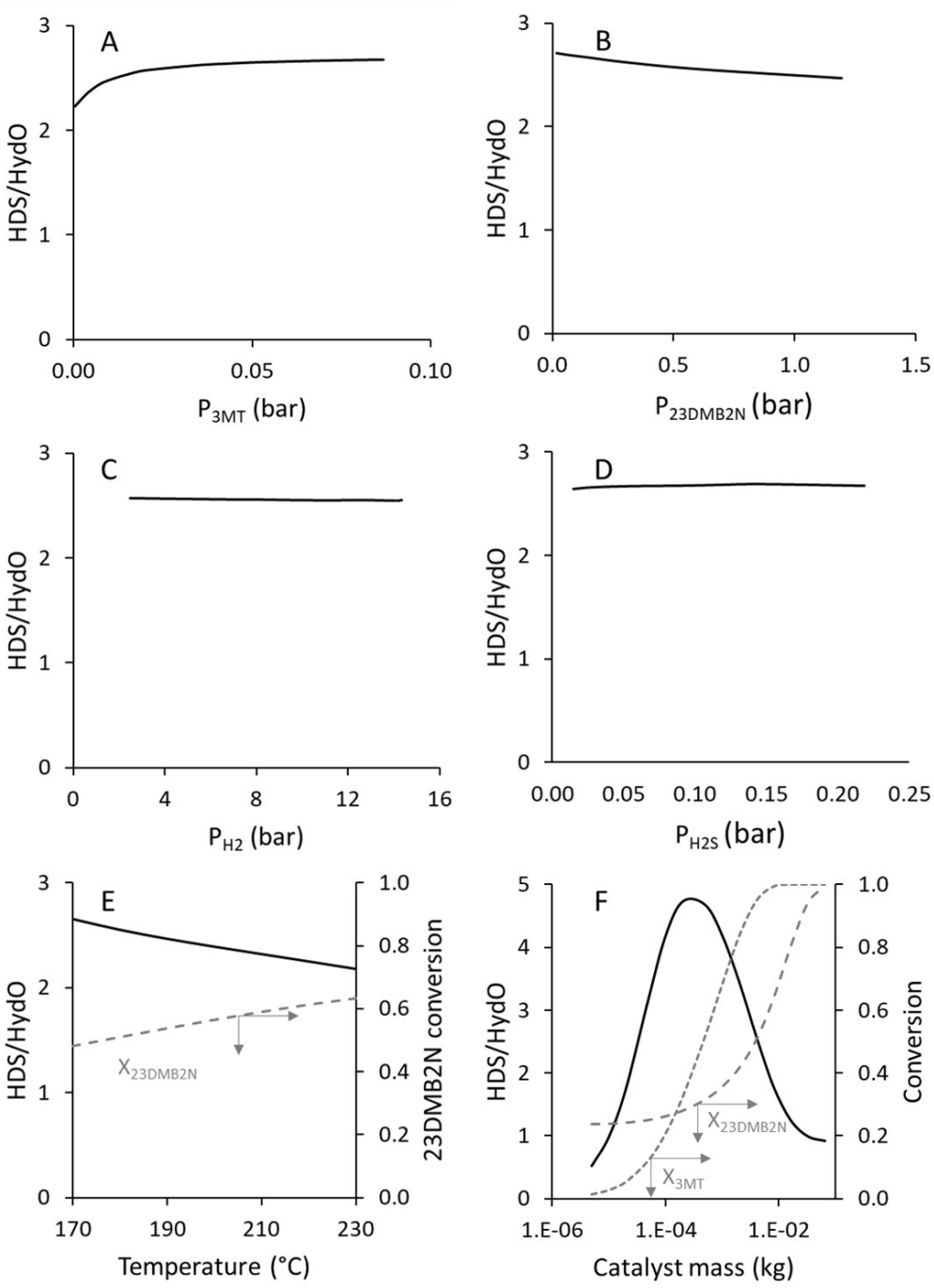

Figure S9. *Selectivity HDS/HydO as a function of different process variables. A-D: 3MT conversion equals 0.95 and 23DMB2N conversion equals 0.51 at reactor outlet, 180°C. E: 3MT conversion equals 0.95 at reactor outlet. F: 180°C.*
Default operating conditions: 0.33 wt% 3MT, 10 wt% 23DMB2N over $CoMo/Al_2O_3$ at 15 bar, LHSV of 3 h^{-1}, H_2/feedstock ratio of 300 $NL.L^{-1}$, 180°C.

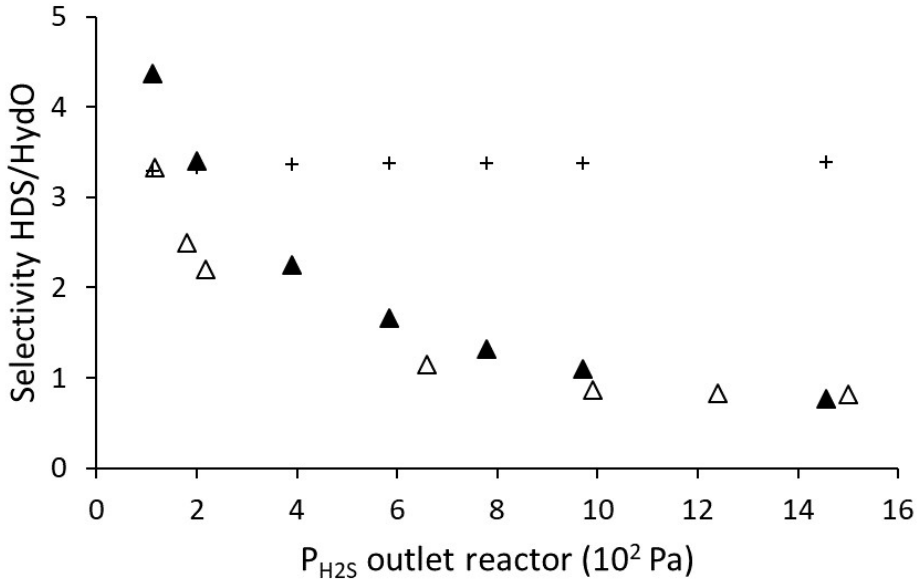

Figure S10. *Selectivity HDS/HydO as a function of the partial pressure of H_2S. Open symbols (❒) data extracted from Figure 13 in [9]. Closed symbols (❑) model simulations at constant contact time. (+) 3MT conversion equals 10% at reactor outlet by varying the contact time.*

Table S4: *Parameter correlation coefficient matrix. Parameter estimates given in Table 3 and 4 of the manuscript.*

	k_5	k_6	K_7	k_8	K_9	k_{10}	k_{-10}	k_{11}	k_{-11}	k_{12}	k_{13}	k_{14}	k_{15}	k_{16}	K_2	K_4	E_5	E_6	ΔH_7	E_8	ΔH_9	E_{10}	E_{11}	E_{12}	E_{13}	E_{14}	E_{15}	E_{16}
k_5	1.00	**0.93**	-0.14	-0.13	-0.23	0.01	0.02	0.03	0.03	-0.05	0.03	-0.06	0.56	0.56	0.89	0.83	0.14	0.10	0.07	0.15	0.14	0.08	0.05	0.14	0.02	0.05	0.21	0.22
k_6	**0.93**	1.00	0.04	-0.07	-0.33	0.04	0.05	0.04	0.02	-0.01	0.09	-0.01	0.57	0.63	0.88	0.83	0.24	0.03	-0.09	0.11	0.20	0.07	-0.02	0.14	-0.02	0.05	0.19	0.16
K_7	-0.14	0.04	1.00	0.59	-0.26	-0.15	-0.08	0.21	0.16	-0.07	0.26	0.10	-0.04	0.03	-0.12	0.02	0.07	-0.08	-0.86	-0.48	0.17	0.21	-0.20	0.19	-0.15	0.08	0.04	0.01
k_8	-0.13	-0.07	0.59	1.00	0.00	0.07	0.11	0.05	0.07	-0.23	0.20	-0.15	0.09	0.01	-0.19	-0.08	-0.10	-0.08	-0.51	-0.89	-0.02	-0.04	0.05	0.21	-0.15	0.11	-0.04	-0.02
K_9	-0.23	-0.33	-0.26	0.00	1.00	-0.08	-0.05	0.16	0.15	0.08	-0.10	-0.18	-0.38	-0.47	-0.21	-0.18	-0.06	0.09	0.28	-0.01	-0.61	0.02	-0.07	-0.10	0.08	0.02	0.11	0.20
k_{10}	0.01	0.04	-0.15	0.07	-0.08	1.00	**0.90**	-0.38	-0.36	0.16	-0.06	0.05	-0.03	-0.01	-0.01	-0.01	0.01	0.03	0.04	-0.08	-0.03	-0.75	0.01	0.01	-0.02	0.09	0.03	0.07
k_{-10}	0.02	0.05	-0.08	0.11	-0.05	**0.90**	1.00	-0.33	-0.33	0.04	0.17	0.05	-0.05	-0.03	0.03	0.03	0.07	0.07	-0.04	-0.11	-0.06	-0.58	-0.11	0.08	-0.23	0.07	0.07	0.13
k_{11}	0.03	0.04	0.21	0.05	0.16	-0.38	-0.33	1.00	**0.99**	-0.18	-0.10	-0.24	0.04	0.04	0.06	0.15	-0.01	0.06	-0.01	-0.01	-0.01	0.17	0.17	0.02	0.15	-0.07	0.06	0.04
k_{-11}	0.03	0.02	0.16	0.07	0.15	-0.36	-0.33	**0.99**	1.00	-0.23	-0.19	-0.31	0.09	0.06	0.03	0.13	-0.06	0.04	0.04	-0.02	0.00	0.14	0.30	0.05	0.22	-0.04	0.02	0.00
k_{12}	-0.05	-0.01	-0.07	-0.23	0.08	0.16	0.04	-0.18	-0.23	1.00	-0.14	0.46	-0.11	0.00	-0.12	-0.03	0.00	-0.06	0.01	0.24	-0.04	-0.06	-0.26	-0.40	0.15	0.02	-0.01	-0.03
k_{13}	0.03	0.09	0.26	0.20	-0.10	-0.06	0.17	-0.10	-0.19	-0.14	1.00	-0.11	-0.08	-0.05	0.13	0.10	0.20	0.08	-0.28	-0.19	0.04	0.22	-0.46	0.12	-0.85	0.07	0.11	0.12
k_{14}	-0.06	-0.01	0.10	-0.15	-0.18	0.05	0.05	-0.24	-0.31	0.46	-0.11	1.00	-0.10	-0.01	-0.04	-0.06	0.06	-0.05	-0.15	0.13	0.10	0.02	-0.38	-0.23	0.08	-0.28	0.00	-0.04
k_{15}	0.56	0.57	-0.04	0.09	-0.38	-0.03	-0.05	0.04	0.09	-0.11	-0.08	-0.10	1.00	**0.93**	0.46	0.65	0.21	0.12	0.01	0.07	0.23	0.22	0.30	0.43	0.22	0.32	-0.14	-0.17
k_{16}	0.56	0.63	0.03	0.01	-0.47	-0.01	-0.03	0.04	0.06	0.00	-0.05	-0.01	**0.93**	1.00	0.53	0.68	0.31	0.12	-0.07	0.12	0.29	0.19	0.19	0.34	0.19	0.26	-0.09	-0.20

K_2	0.89	0.88	-0.12	-0.19	-0.21	-0.01	0.03	0.06	0.03	-0.12	0.13	-0.04	0.46	0.53	1.00	0.85	0.43	0.25	0.05	0.17	0.13	0.08	-0.09	0.09	-0.10	-0.04	0.26	0.25
K_4	0.83	0.83	0.02	-0.08	-0.18	-0.01	0.03	0.15	0.13	-0.03	0.10	-0.06	0.65	0.68	0.85	1.00	0.51	0.34	-0.07	0.23	0.11	0.26	0.00	0.43	0.08	0.30	0.27	0.28
E_5	0.14	0.24	0.07	-0.10	-0.06	0.01	0.07	-0.01	-0.06	0.00	0.20	0.06	0.21	0.31	0.43	0.51	1.00	0.43	-0.20	0.17	0.04	0.34	-0.23	0.44	-0.09	0.34	0.24	0.19
E_6	0.10	0.03	-0.08	-0.08	0.09	0.03	0.07	0.06	0.04	-0.06	0.08	-0.05	0.12	0.12	0.25	0.34	0.43	1.00	0.18	0.20	-0.28	0.14	-0.03	0.25	0.07	0.24	0.34	0.61
ΔH_7	0.07	-0.09	-0.86	-0.51	0.28	0.04	-0.04	-0.01	0.04	0.01	-0.28	-0.15	0.01	-0.07	0.05	-0.07	-0.20	0.18	1.00	0.42	-0.33	-0.27	0.30	-0.29	0.23	-0.13	-0.10	0.01
E_8	0.15	0.11	-0.48	-0.89	-0.01	-0.08	-0.11	-0.01	-0.02	0.24	-0.19	0.13	0.07	0.12	0.17	0.23	0.17	0.20	0.42	1.00	0.01	0.21	0.03	0.00	0.31	0.15	0.15	0.08
ΔH_9	0.14	0.20	0.17	-0.02	-0.61	-0.03	-0.06	-0.01	0.00	-0.04	0.04	0.10	0.23	0.29	0.13	0.11	0.04	-0.28	-0.33	0.01	1.00	0.09	0.10	0.11	-0.06	-0.12	-0.37	-0.47
E_{10}	0.08	0.07	0.21	-0.04	0.02	-0.75	-0.58	0.17	0.14	-0.06	0.22	0.02	0.22	0.19	0.08	0.26	0.34	0.14	-0.27	0.21	0.09	1.00	-0.05	0.45	-0.03	0.35	0.03	0.01
E_{11}	0.05	-0.02	-0.20	0.05	-0.07	0.01	-0.11	0.17	0.30	-0.26	-0.46	-0.38	0.30	0.19	-0.09	0.00	-0.23	-0.03	0.30	0.03	0.10	-0.05	1.00	0.29	0.58	0.36	-0.37	-0.26
E_{12}	0.14	0.14	0.19	0.21	-0.10	0.01	0.08	0.02	0.05	-0.40	0.12	-0.23	0.43	0.34	0.09	0.43	0.44	0.25	-0.29	0.00	0.11	0.45	0.29	1.00	0.10	0.73	-0.03	0.08
E_{13}	0.02	-0.02	-0.15	-0.15	0.08	-0.02	-0.23	0.15	0.22	0.15	-0.85	0.08	0.22	0.19	-0.10	0.08	-0.09	0.07	0.23	0.31	-0.06	-0.03	0.58	0.10	1.00	0.22	-0.10	-0.11
E_{14}	0.05	0.05	0.08	0.11	0.02	0.09	0.07	-0.07	-0.04	0.02	0.07	-0.28	0.32	0.26	-0.04	0.30	0.34	0.24	-0.13	0.15	-0.12	0.35	0.36	0.73	0.22	1.00	0.05	0.11
E_{15}	0.21	0.19	0.04	-0.04	0.11	0.03	0.07	0.06	0.02	-0.01	0.11	0.00	-0.14	-0.09	0.26	0.27	0.24	0.34	-0.10	0.15	-0.37	0.03	-0.37	-0.03	-0.10	0.05	1.00	0.82
E_{16}	0.22	0.16	0.01	-0.02	0.20	0.07	0.13	0.04	0.00	-0.03	0.12	-0.04	-0.17	-0.20	0.25	0.28	0.19	0.61	0.01	0.08	-0.47	0.01	-0.26	0.08	-0.11	0.11	0.82	1.00

References

[1] E. Krebs, B. Silvi, A. Daudin, P. Raybaud, A DFT study of the origin of the HDS/HydO selectivity on Co(Ni)MoS active phases, J. Catal. 260 (2008) 276–287. https://doi.org/10.1016/j.jcat.2008.09.026.

[2] J. P. Perdew, Y. Wang, Accurate and simple analytic representation of the electron-gas correlation energy, Phys. Rev. B 45 (1992) 13244. https://doi.org/10.1103/PhysRevB.45.13244

[3] J. P. Perdew, J. A. Chevary, S. H. Vosko, K. A. Jackson, M. R. Pederson, D. J. Singh, C. Fiolhais, Atoms, molecules, solids, and surfaces: Applications of the generalized gradient approximation for exchange and correlation, Phys. Rev. B 46 (1992) 6671. https://doi.org/10.1103/PhysRevB.46.6671

[4] G. Kresse, J. Furthmüller, Efficiency of ab-initio total energy calculations for metals and semiconductors using a plane-wave basis set, Comput. Mater. Sci. 6 (1996) 15-50. https://doi.org/10.1016/0927-0256(96)00008-0

[5] G. Kresse, J. Furthmüller, Efficient iterative schemes for ab initio total-energy calculations using a plane-wave basis set, Phys. Rev. B 54 (1996) 11169. https://doi.org/10.1103/PhysRevB.54.11169

[6] G. Kresse, D. Joubert, From ultrasoft pseudopotentials to the projector augmented-wave method, Phys. Rev. B 59 (1999) 1758. https://doi.org/10.1103/PhysRevB.59.1758

[7] B. Baubet, M. Girleanu, A.-S. Gay, A.-L. Taleb, M. Moreaud, F. Wahl, V. Delattre, E. Devers, A. Hugon, O. Ersen, P. Afanasiev, P. Raybaud, Quantitative Two-Dimensional (2D) Morphology–Selectivity Relationship of CoMoS Nanolayers: A Combined High-Resolution High-Angle Annular Dark Field Scanning Transmission Electron Microscopy (HR HAADF-STEM) and Density Functional Theory (DFT) Study, ACS Catal. 6 (2016) 1081–1092. https://doi.org/10.1021/acscatal.5b02628.

[8] P. Atkins, Physical Chemistry, 6th edition 2000, W.H. Freeman and Company, New York

[9] N. Dos Santos, H. Dulot, N. Marchal, M. Vrinat, New insight on competitive reactions during deep HDS of FCC gasoline, Appl. Catal. A: Gen. 352 (2009) 114–123. https://doi.org/10.1016/j.apcata.2008.09.035.